Available online at www.sciencedirect.com
ScienceDirect
International Journal of Heat and Mass Transfer 50 (2007) 513–529
International Journal of HEAT and MASS TRANSFER
www.elsevier.com/locate/ijhmt

An investigation on spill plume development and natural filling in large full-scale atrium under retail shop fire

C.L. Shi [a,d], W.Z. Lu [b,*], W.K. Chow [c], R. Huo [d]

[a] China Academy of Safety Sciences and Technology, State Administration of Work Safety, Beijing 100029, China
[b] Department of Building and Construction, City University of Hong Kong, Kowloon Tong, Kowloon, Hong Kong, China
[c] Department of Building Services Engineering, The Hong Kong Polytechnic University, Hong Kong, China
[d] State Key Laboratory of Fire Science, University of Science and Technology of China, Hefei 230026, China

Received 12 November 2004; received in revised form 18 August 2005
Available online 28 September 2006

Abstract

This paper reports an investigation on the scenarios of the spill plume and the resultant natural filling in a full-scale atrium mock-up due to a retail shop fire. The study includes two aspects, i.e., the full-scale experiment and the numerical simulation. A spill plume model is proposed to predict the characteristic properties of the plume development in the atrium under a retail shop fire. Furthermore, to accurately predict the shop fire in the atrium, an improved zone model is developed combining the transport lag time model and the spill plume model. Besides validating the developed model by experiments, the case is also simulated by the established zone model, i.e., CFAST code, and the computational fluid dynamics model, i.e., FDS code. By both physical and numerical experiments, the process of natural smoke filling and the temperature rise in the atrium are investigated and well understood. It is found that a typical spill plume contains three regimes, i.e., the curved section out of the retail shop door, the line plume in the near field, and the axisymmetric plume in the far field. Predictions from the proposed empirical model for the spill plume and the resultant improved zone model compare favorably with the experiments. The study indicates that the atrium becomes very dangerous due to such shop fire if no smoke control employed. The ability of mechanical exhaust system in the atrium to mitigate the hazard of a retail shop fire is investigated as well.

Keywords: Atrium; Shop fire; Spill plume; Zone model; Natural filling; Mechanical exhaust

1. Introduction

Today, large-scale shopping malls/atria become normal in many metropolitan cities like Hong Kong, Beijing, Shanghai, Tokyo, etc., in which, many retail shops are constructed in different levels. The safety under emergency is of first priority in such public locations, especially in case of fire. Fire originating in a retail shop is likely to generate large mount of smoke dispersing into the atrium and spreading to other levels rapidly due to the open design feature. Hence, to achieve an effective atrium smoke control design, it is necessary to thoroughly investigate the fire scenario from a retail shop located inside the atrium, e.g., the entrainment of the spill plume, the natural filling process, etc.

Traditionally, the spill plume of fire is treated either as a virtual origin line plume, e.g., the balcony spill plume, in most design guidelines [1–3] or axisymmetric plume [4–6] in zone model, e.g., CFAST [6], a well established zone model code. There are some empirical correlations to predict the entrainment of the spill plume [5,7,8], but give no detailed description on the transition of the near line plume to the far field axisymmetric plume. In fact, for the case of retail shop fire in large atrium, the smoke spilling out of the shop door into a tall atrium usually develops into three typical regimes, i.e., the horizontal curved section at the door, the line plume in the near field, and the final axisym-

* Corresponding author. Tel.: +852 27844316; fax: +852 27887612.
E-mail address: bcwzlu@cityu.edu.hk (W.Z. Lu).

0017-9310/$ - see front matter © 2006 Elsevier Ltd. All rights reserved.
doi:10.1016/j.ijheatmasstransfer.2006.07.020

Nomenclature

$A_{c,s}$	area of shop ceiling
$A_{c,a}$	area of atrium ceiling
A_g	surface area of smoke layer
$A_{w,j}$	area of surface j
b	half width of plume
B	$g/c_pT_0\rho_0$
c_p	specific heat of air at constant pressure
C_m	dimensionless entrainment coefficient
D_f	diameter of fire source
g	acceleration of gravity
G_r	Grashof number
h	effective heat transfer coefficient
h_j	heat transfer coefficient of surface j
$h_{c,j}$	convective heat transfer coefficient of surface j
h_o	heat transfer coefficient of outside surface
H_a	height of atrium
H_d	height of door
H_n	height of neutral plane
H_s	height of shop
i	number of thin element of wall
k	thermal conductivity
k_g	absorption coefficient of smoke layer
k_m	spill plume profile factor for mass flux
k_Q	spill plume profile factor for heat flux
l	characteristic length
L_m	mean beam length
$m_{g,a}$	total mass of smoke layer in atrium
$m_{g,s}$	total mass of smoke layer in shop
$\dot{m}_f$	mass loss rate of fire source
$\dot{m}_i$	mass exchange rate at interface
$\dot{m}_p$	mass flow rate of plume
$\dot{m}_{p,l}$	mass flow rate of line plume
$\dot{m}_{p,a}$	mass flow rate of axisymmetric plume
$\dot{m}_v$	mass flow rate out of door
n	time steps
p	growth power of t^p fire
P	pressure
P_r	Prandtl number
$\dot{Q}$	total heat release rate
$\dot{Q}_a$	heat flux of axisymmetric plume
$\dot{Q}_c$	convective heat release rate
$\dot{Q}_d$	heat flux of plume at door height
$\dot{Q}_l$	heat flux of line plume
$\dot{Q}_v$	heat flow rate out of door
$\dot{Q}_L$	heat loss rate
r	radius
t	time
t_{lag}	transport lag time
t_{out}	time when the smoke flows out
t_p^*	normalized time for t^p fire
T_0	ambient temperature
$T_{0,a}$	initial temperature of atrium
$T_{0,s}$	initial temperature of shop
$T_{0,w}$	initial temperature of wall
T_g	temperature of smoke layer
$T_{g,a}$	smoke layer temperature in atrium
$T_{g,s}$	smoke layer temperature in shop
T_m	centerline temperature of plume
$T_{w,j}$	temperature of inner surface j
u	velocity
w_m	centerline velocity of plume
W	width of door
Z	height
Z_o	virtual origin
$Z_{o,a}$	virtual origin of axisymmetric plume
$Z_{o,l}$	virtual origin of line plume
Z_b	elevation of fire bottom
Z_{fl}	height of flame
$Z_{l,a}$	critical transition height
$Z_{g,a}$	height of smoke layer in atrium
$Z_{g,s}$	height of smoke layer in shop

Greek symbols

α	thermal diffusivity of wall
α_c	fire growth coefficient
χ	combustion efficiency
δ	thickness of wall
$\varepsilon_{g,a}$	smoke emissivity in atrium
$\varepsilon_{g,s}$	smoke emissivity in shop
ε_w	emissivity of wall
κ	coefficient in Eq. (51)
λ_c	coefficient of convective HRR
ν	kinematic viscosity of air
ρ	density
ρ_0	density of ambient air
$\rho_{0,a}$	air density in atrium
$\rho_{0,s}$	air density in shop
ρ_g	density of plume
$\rho_{g,s}$	density of hot smoke in shop
σ	Stefan–Boltzman constant
ΔH_c	heat of combustion

metric plume formed above the shop. The entrainment rates and the temperature distributions of the plume are different for these regimes. Hence, a single linear or axisymmetric plume model for the whole region of the plume is not appropriate. Thomas [7] and Heskestad [5] have developed their one-equation correlation for the entrainment of a similar spill plume; however, they did not consider the different virtual origin for the sections of the line plume and the axisymmetric plume, and did not notice the effect of the spill depth at the door on the critical transition height. For example, if the depth is approximated to be equal to the width of the door or the balcony, the spill

plume may just be approximately an axisymmetric plume after it flows out.

At present, there are still few zone models able to simulate a retail shop fire in a large, tall atrium. First the spill plume is often treated as an axisymmetric plume without respect to the spill plume transition characteristics. Second axisymmetric plume models usually have a height limit. McCaffrey's correlation [9] in CFAST may predict mass entrainment rates of the plume almost twice those of Zukoski's [10] and Heskestad's [11] equations at the height of 20 m above the fire source with heat release rate of 500 kW. Finally, the transport time, which plays a key role in the formation of smoke layer, is seldom considered in current zone models [6,12].

This paper reports a detailed investigation of full-scale fire growth and smoke movement in an atrium due to a retail shop fire through both physical experiments and numerical simulations. Previous studies [2,3] on such fires were mainly carried out by scaled, physical models because the full-scale burning test is always expensive and time-consuming. In this study, full-scale retail shop fires were performed in an atrium constructed in the University of Science and Technology of China (USTC), Hefei, Anhui, China, as a collaboration project with The Hong Kong Polytechnic University (PolyU). Two full-scale burning tests were carried out in the retail shop mock-up located inside the PolyU/USTC Atrium [13]. Numerical simulations were performed by the computational fluid dynamics model, i.e., Fire Dynamics Simulator, FDS [14]. A simplified spill plume model was proposed to predict the characteristic properties of the spill plume and results are compared to the available measured data and simulation by FDS. An improved zone model was also developed to simulate the retail shop fire in an atrium, including the spill plume model and a calculating method of the transport lag time in the code. Through both physical and numerical experiments, the process of natural smoke filling and the temperature rise in the atrium are expected to be understood further. The factors affecting the numerical accuracy are analyzed. Finally, by prediction of the present zone model, the efficiency of a mechanical exhaust system installed in the atrium submitted to retail shop fires is investigated.

2. Proposed model for spill plume out of a wide shop door

2.1. Horizontal curved section of the spill plume

Smoke movement inside the whole environment due to a retail shop fire is illustrated in Fig. 1. Inside the enclosure of the retail shop, the heat and mass are transferred from fire source to the upper layer by the near field axisymmetric plume. A hot smoke layer forms and descends to spill out of the shop. The flow rates of heat ($\dot{Q}_v$) and mass ($\dot{m}_v$) out of the shop can be defined by the following integrations [15]:

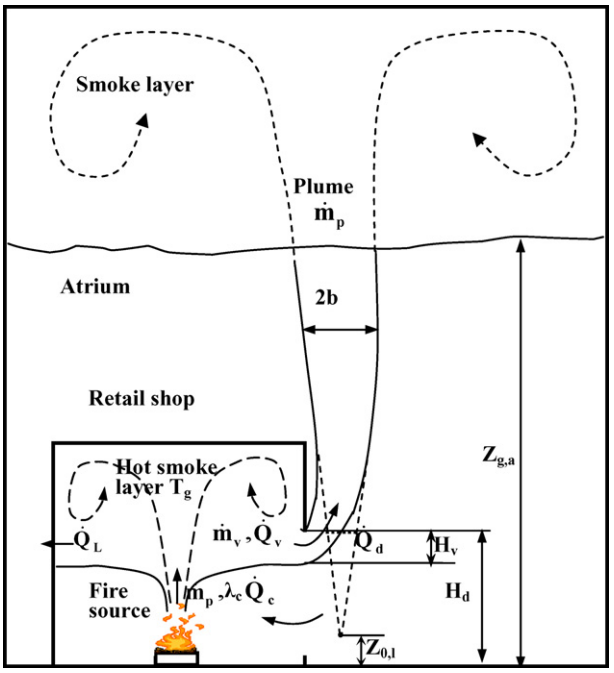

Fig. 1. Spill plume due to a retail shop fire in atrium.

$$\dot{Q}_v = \rho_0 c_p T_0 W \int_{H_v} \left(1 - \frac{T_0}{T_g}\right) u \, dz = \frac{2\sqrt{2g}}{3} (k_Q/k_m) \rho_c c_p H_v^{3/2} W (T_g - T_0)^{3/2} T_0^{-1/2} \quad (1)$$

$$\dot{m}_v = \rho_0 W \int_{H_v} \left(\frac{T_0}{T_g}\right) u \, dz = \frac{2\sqrt{2g}}{3k_m} \rho_c H_v^{3/2} W (T_g - T_0)^{1/2} T_0^{-1/2} \quad (2)$$

in which, ρ_0 and T_0 are the ambient air density and temperature, ρ_g and T_g are the density and temperature of the hot smoke, g is the acceleration of gravity, W is the width of the door, H_v is the spill plume depth at the door, k_Q and k_m are the profile factor coefficients.

Concerning energy and mass conservation, the $\dot{Q}_v$ and $\dot{m}_v$ can also be expressed as:

$$\dot{Q}_v = \dot{Q}_c - \dot{Q}_L = \lambda_c \dot{Q} - h A_g (T_g - T_0) \quad (3)$$

$$\dot{m}_v = \dot{m}_p \quad (4)$$

where $\dot{Q}_c = \lambda_c \dot{Q}$ is defined as the convective heat output of the fire source and $\dot{Q}_L$ is the heat loss rate of the smoke layer to the boundary, h is the effective heat transfer coefficient, A_g is the surface area of the smoke layer. $\dot{m}_p$ is the mass flow rate into the upper layer in retail shop. For far field conditions, $\dot{m}_p$ takes the following formation [11]:

$$\dot{m}_p = 0.071 \dot{Q}_c^{1/3} [H_d - 1.1 H_v - (0.083 \dot{Q}^{2/5} - 1.02 D_f) - Z_b]^{5/3} + 0.0018 \dot{Q}_c \quad (5)$$

For the near field of the fire plume region, it becomes:

$$\dot{m}_p = 0.0054 \dot{Q}_c [H_d - 1.1 H_v - Z_b] / Z_{fl} \quad (6)$$

$$Z_{fl} = -1.02 D_f + 0.235 \dot{Q}^{2/5} \quad (7)$$

where H_d is the door height, Z_{fl} is the flame height, Z_b is the elevation of the fire bottom. D_f is fire diameter.

2.2. Near field of the spill plume

The near field of the plume outside the shop can be approximated as a line plume, originated from the virtual fire source $Z_{o,l}$ shown in Fig. 1. Hence, the mass flow rate and the centerline temperature can be described by a two-dimensional line plume. An unbounded line thermal plume model is developed by Lee and Emmons [16], as:

$$\dot{m}_{p,l}/W = C_m \rho [g(\dot{Q}_l/W)/\rho c_p T_0]^{1/3}(Z - Z_{o,l}) \tag{8}$$

where $\dot{m}_{p,l}$ is the mass flow rate, $\dot{Q}_l$ is the heat release rate of virtual line fire, Z is the distance measured from the floor, and C_m is a constant, taken as 0.51 [17] in the study. The above equation is convenient if re-written in the following form:

$$\dot{m}_{p,l} = 0.3 C_m \rho_0 W^{2/3}(\rho/\rho_0)^{2/3}\dot{Q}_l^{1/3}(Z - Z_{o,l}) \tag{9}$$

For large values of Z and for weak plumes, the item $(\rho/\rho_0)^{2/3}$ is close to 1. Thus, Eq. (9) becomes:

$$\dot{m}_{p,l} = 0.3 C_m \rho_0 W^{2/3}\dot{Q}_l^{1/3}(Z - Z_{o,l}) \tag{10}$$

The heat release rate of the virtual fire origin, at steady state, should be the same as the heat flow rate of plume at the door height of the shop, denoted as $\dot{Q}_d$, thus,

$$\dot{Q}_l = \dot{Q}_d \tag{11}$$

An assumption is introduced that the entrainment rate at the curved section of the spill plume is equivalent to that at the section of the line plume from H_d down to $H_d - H_v$ with ignoring the radiation loss. According to energy conservation, the heat release rate of a line virtual source can be written as:

$$\dot{Q}_l = \dot{Q}_d = \dot{Q}_v \tag{12}$$

The virtual origin $Z_{o,l}$ can be obtained by the following equation:

$$\dot{m}_v = 0.3 C_m \rho_0 W^{2/3}\dot{Q}_v^{1/3}(H_d - H_v - Z_{o,l}) \tag{13}$$

The horizontal width of the spill plume at the door height is about $\sqrt{2}H_v$.

Therefore, the near field of the smoke plume outside the shop can be described by the line plume by substituting the heat and mass flow rate of the spill plume at the door opening. Besides the mass entrainment rate given by Eq. (9), the other characteristic parameters of the near field of the smoke plume, characterized as the half width b, the centerline velocity and temperature w_m and T_m, can be given by the following equations, according to the dimensional analysis of Quintiere et al. [18], by substituting the heat release rate $\dot{Q}_v$ and the virtual origin $Z_{o,l}$ as below:

$$b = 0.103(Z - H_d) + \left(\sqrt{2}/2\right)H_v \tag{14}$$

$$w_m = 2.3\left[g\left(\frac{\dot{Q}_v/W}{\rho_0 c_p T_0 g^{1/2}}\right)^{2/3}\right]^{1/2} = 0.7(\dot{Q}_v/W)^{1/3} \tag{15}$$

$$\frac{T_m - T_0}{T_0} = 3.3\left(\frac{\dot{Q}_v/W}{\rho_0 c_p T_0 g^{1/2}}\right)^{2/3}(Z - Z_{o,l})^{-1} = 0.0307(\dot{Q}_v/W)^{2/3}(Z - Z_{o,l})^{-1} \tag{16}$$

2.3. Far field of the spill plume

As the spill plume rises up to the far field, the edge effects need to be considered. Above a critical transition height, the spill plume can be described as an axisymmetric plume. At the critical transition height, the line plume is increased to be equal to the character length, which is defined by the radius of the axisymmetric plume, assumed to be $\sqrt{2}(W/2)$. According to the Eq. (14), this implies

$$b = 0.103(Z_{l,a} - H_d) + \left(\sqrt{2}/2\right)H_v = \left(\sqrt{2}/2\right)W \tag{17}$$

The critical height $Z_{l,a}$ can be obtained by the following equation:

$$Z_{l,a} = H_d + 6.8(W - H_v) \tag{18}$$

As mentioned above, the far field of the spill plume can be described by the axisymmetric plume model [10]. Assuming that the axisymmetric plume is generated by the virtual origin $Z_{o,a}$ with a heat release rate $\dot{Q}_a$, the mass flow rate of the spill plume above the critical transition height may be expressed as:

$$\dot{m}_{p,a} = 0.21\rho_0\sqrt{g(Z - Z_{o,a})^5}\left(\dot{Q}_a/\rho_0 c_p T_0\sqrt{g(Z - Z_{o,a})^5}\right)^{1/3} = 0.063\rho_0\dot{Q}_a^{1/3}(Z - Z_{o,a})^{5/3} \tag{19}$$

where $\dot{Q}_a$ is the heat flow rate at the transition height $Z_{l,a}$, as in the near field,

$$\dot{Q}_a = \dot{Q}_l = \dot{Q}_v \tag{20}$$

and $Z_{o,a}$ may be obtained by the following equation at the transition height:

$$\dot{m}_{p,a}|_{z=z_{l,a}} = \dot{m}_{p,l}|_{z=z_{l,a}} \tag{21}$$

Thus

$$Z_{o,a} = Z_{l,a} - \left[4.76 C_m W^{2/3}(Z_{l,a} - Z_{o,l})\right]^{3/5} \tag{22}$$

The other characteristics of the far field of the spill plume are determined by dimensional analysis [10] as:

$$b = 0.131(Z - Z_{o,a} - \Delta Z_{o,b}) \tag{23}$$

$$w_m = 1.169\dot{Q}_v^{1/3}(Z - Z_{o,a} - \Delta Z_{o,w})^{-1/3} \tag{24}$$

$$\frac{T_m - T_0}{T_0} = 9.115(\rho_0 c_p T_0 g^{1/2})^{-2/3}\dot{Q}_v^{2/3}(Z - Z_{o,a} - \Delta Z_{o,T})^{-5/3} = 0.0849\dot{Q}_v^{2/3}(Z - Z_{o,a} - \Delta Z_{o,T})^{-5/3} \tag{25}$$

3. Proposed zone model for retail shop fire in a large atrium

To study the retail shop fire in a large atrium, the zone model is an easy, simple approach for modeling the smoke and heat movement. However, to date, the majority of zone models have inherent limitation due to the properties of the spill plume described by different axisymmetric plume models with different applicability limits, and the neglect of transport lag time to form a smoke layer in the atrium. In this study, we developed an improved zone model to simulate the retail shop fire in an atrium, which includes a new spill plume model and the transport lag time concurrently.

3.1. Smoke and heat movement in retail shop

The retail shop under fire can be generally divided into two regions [12,19], i.e., the upper smoke layer and the lower cool layer. Fig. 2 presents the basic phenomena and the relevant terminology of fire in the shop. The physical properties in these two regions are assumed to be uniformly distributed. Taking the retail shop air pressure to be the same as the ambient pressure P_0, the mass and heat balances of the smoke layer are given by the following equations:

$$\frac{dm_{g,s}}{dt} = \dot{m}_p + \dot{m}_i + \dot{m}_f - \dot{m}_v \tag{26}$$

$$\frac{dm_{g,s}c_pT_{g,s}}{dt} = \lambda_c\dot{Q} - \dot{Q}_L + (\dot{m}_i + \dot{m}_p + \dot{m}_f)c_pT_{0,s} - \dot{m}_vc_pT_{g,s} \tag{27}$$

where $m_{g,s}$ and $T_{g,s}$ are the mass and temperature of the hot smoke layer in the shop. $\dot{m}_v$ is the mass flow rate out of the vent. The smoke production rate from the fire source $\dot{m}_f$ and mass exchange rate at the interface of the two zones $\dot{m}_i$ are usually small comparing with the mass entrainment rate into the plume $\dot{m}_p$ and can be neglected in most cases. Assuming the air to be ideal gases, the resultant transient equations for the smoke layer height $Z_{g,s}$ and temperature $T_{g,s}$ can be given by:

$$\frac{dZ_{g,s}}{dt} = \frac{(\dot{m}_v - \dot{m}_p)}{\rho_{g,s}A_{c,s}} - \frac{\lambda_c\dot{Q} - \dot{Q}_L - \dot{m}_pc_p(T_{g,s} - T_{0,s})}{\rho_{0,s}T_{0,s}c_pA_{c,s}} \tag{28}$$

$$\frac{dT_{g,s}}{dt} = \frac{\lambda_c\dot{Q} - \dot{Q}_L - \dot{m}_pc_p(T_{g,s} - T_{0,s})}{\rho_{g,s}c_p(H_s - Z_{g,s})} \tag{29}$$

in which $A_{c,s}$ and H_s are the ceiling area and height of the shop.

The heat loss rate $\dot{Q}_L$, through all boundary surfaces of the shop enclosure due to radiation and convection, can be specified as follows:

$$\dot{Q}_L = \sum h_jA_{w,j}(T_{g,s} - T_{w,j}) \tag{30}$$

where $A_{w,j}$ is the area of surface j and $T_{w,j}$ is the inner surface temperature. h_j is the total heat transfer coefficient, given by

$$h_j = \frac{\varepsilon_{g,s}\varepsilon_w}{\varepsilon_{g,s} + \varepsilon_w - \varepsilon_{g,s}\varepsilon_w}\sigma(T_{g,s}^2 + T_{w,j}^2)(T_{g,s} + T_{w,j}) + h_{c,j} \tag{31}$$

where ε_w is the emissivity of the wall boundary. $\varepsilon_{g,s}$, the emissivity of the smoke layer, can be estimated by

$$\varepsilon_{g,s} = 1 - \exp(-k_gL_m) \tag{32}$$

k_g, the absorption coefficient of the smoke layer, has different values for different fuels, and is 0.43 m^{-1} for diesel fuel [20]. L_m is the mean beam length, defined below

$$L_m = \frac{4A_{c,s}(H_s - Z_{g,s})}{[2A_{c,s} + 4(H_s - Z_{g,s})\sqrt{A_{c,s}}]} \tag{33}$$

The convective heat transfer coefficient $h_{c,j}$ for turbulent, natural convection is expressed as a function of P_r, the Prandtl number (0.72 for air) and G_r, the Grashof number, which changes with the boundary surfaces as below [6]:

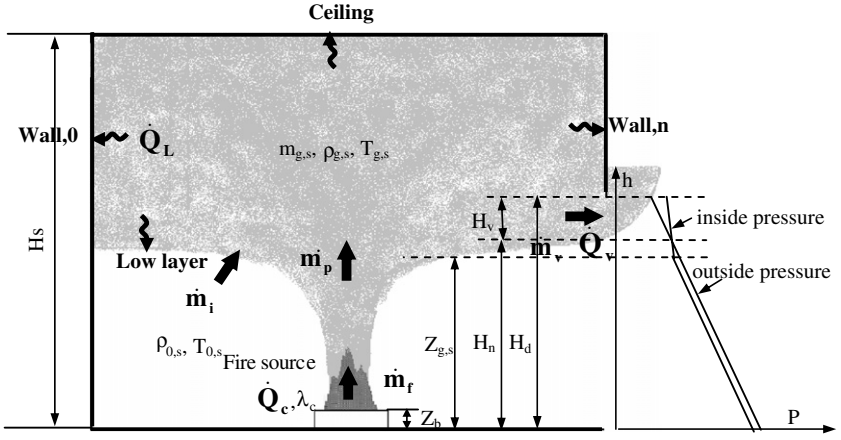

Fig. 2. Schematic of terms and processes associated with retail shop fire.

$$h_{c,j}=\begin{cases}0.21\dfrac{k}{l}(G_rP_r)^{1/3} & \text{for ceiling}\\ 0.13\dfrac{k}{l}(G_rP_r)^{1/3} & \text{for verical walls}\\ 0.012\dfrac{k}{l}(G_rP_r)^{1/3} & \text{for lower layer and floor}\end{cases} \tag{34}$$

l is the characteristic length scale, $A_{w,j}^{1/2}$. The Grashof number, G_r, thermal conductivity, k, and kinematic viscosity of air, v, are all related to the temperature of the smoke layer and boundary, given by,

$$G_r=\frac{gl^3|T_{g,s}-T_{w,j}|}{v^2T_{g,s}},$$
$$k=2.72\times10^{-7}\left(\frac{T_{g,s}+T_{w,j}}{2}\right)^{4/5},$$
$$v=7.18\times10^{-10}\left(\frac{T_{g,s}+T_{w,j}}{2}\right)^{7/4} \tag{35}$$

To evaluate the heat loss to the enclosure, it is necessary to calculate the wall's inner surface temperature $T_{w,j}$, which changes with the time. A simple, one-dimensional heat transfer calculation is implemented in the study by dividing the wall thickness δ into i thin, parallel elements, shown in Fig. 3. The governing equation are

$$\frac{\partial T_{w,j}}{\partial t}=\alpha\frac{\partial^2T_{w,j}}{\partial x^2} \tag{36}$$

It is solved with the following boundary conditions:

$$T_{w,j}=T_{0,w}\quad \text{at } t=0$$
$$\frac{\partial T_{w,j}}{\partial x}=h_{w,j}(T_{g,s}-T_{w,j})\quad \text{at } x=0$$
$$\frac{\partial T_{w,j,i}}{\partial x}=h_o(T_{w,j,i}-T_{0,a})\quad \text{at } x=\delta$$

where the heat transfer coefficient h_o [21] of the outside surface is given by

$$h_o=3.3\times10^{-5}T_{w,j,i}-3.09\times10^{-4}\ \text{kW/m}^2\ \text{K} \tag{37}$$

The initial value of temperature $T_{0,w}$ of the walls can be different from the initial temperature inside the shop $T_{0,s}$ and atrium $T_{0,a}$.

Currently, several plume models are available for predicting the mass flow rate $\dot{m}_p$ of the plume [10,11,18]. Considering the fire case in a retail shop, Heskestad's model is reckoned a suitable one to calculate the entrainment rate of the plume. The model was based on large-scale experiments involving relatively high heat release rates and realistic fuel packages. The detailed formulations are listed below for the two regions

$$\text{smoke plume region}\begin{cases}\dot{m}_p=0.071\dot{Q}_c^{1/3}(Z_{g,s}-Z_o-Z_b)^{5/3}+0.0018\dot{Q}_c\\ Z_0=0.083\dot{Q}^{2/5}-1.02D_f\end{cases} \tag{38}$$

$$\text{fire plume region}\begin{cases}\dot{m}_p=0.0054\dot{Q}_c(Z_{g,s}-Z_b)/Z_{fl}\\ Z_{fl}=-1.02D_f+0.235\dot{Q}^{2/5}\end{cases} \tag{39}$$

When the hot layer descends to the elevation of the door opening of the shop, the hot smoke will be driven to flow out by the pressure difference across the door opening. Based on Bernoulli's equation, the flow rate of the mass $\dot{m}_v$ and heat $\dot{Q}_v$ out of the door can be derived from the average spill velocity and expressed as

$$\dot{m}_v=\int_{H_v}\rho_{g,s}Wu\,dz=\frac{2}{3k_m}\rho_{g,s}H_v^{3/2}W\sqrt{2g(T_{g,s}-T_{0,a})} \tag{40}$$

$$\dot{Q}_v=\int_{H_v}\rho_{g,s}Wuc_p(T_{g,s}-T_{0,a})\,dz=\frac{2\sqrt{2g}}{3}k_Q/k_m\rho_{g,s}H_v^{3/2}W(T_{g,s}-T_{0,a})^{3/2}T_{0,a}^{-1/2} \tag{41}$$

where k_m and k_Q are coefficients concerning the temperature and the velocity distributions of the outflow. In this study, k_m is assigned to be 1.35 according to the average horizontal outflow velocity measured in the previous experiments, and k_Q is taken as 0.9 considering that the temperature of the spill plume is a little lower than that of the smoke layer inside the shop [15].

The position of the neutral plane, H_n, is located approximately at the height of the soffit of the spill plume at the vent section, and the interface height $Z_{g,s}$ is a little lower than the neutral plane height, i.e.,

$$H_n=H_d-H_v \tag{42}$$
$$Z_{g,s}=H_d-1.1H_v \tag{43}$$

3.2. Smoke spread and natural filling in atrium

Assuming a constant pressure at a given height and neglecting heat expansion, the temperature and the interface height of the smoke layer in the atrium can be calculated by the following set of simultaneous equations:

$$\frac{dZ_{g,a}}{dt}=\frac{\dot{m}_p}{\rho_{g,a}A_{c,a}} \tag{44}$$

$$\frac{dT_{g,a}}{dt}=\frac{\dot{Q}_v-\sum h_jA_{w,j}(T_{g,a}-T_{w,j})-\dot{m}_pc_p(T_{g,a}-T_{0,a})}{\rho_{g,a}c_p(H_a-Z_{g,a})} \tag{45}$$

The variables of the smoke layer with secondary subscript a represent the corresponding quantities in atrium.

Normally the door opening of the retail shop is relatively wide. Hence, it is more suitable to divide the spill plume out of vertical section into two parts, i.e., the line plume in the near field and the axisymmetric plume in the far field, rather than specifying the plume as axisymmetric as in CFAST model. The characteristics of the spill

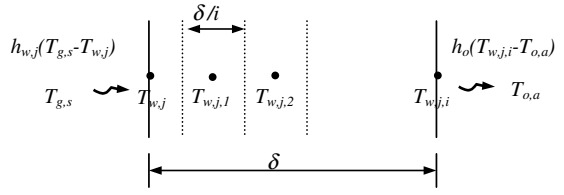

Fig. 3. Numerical method solving transient heat conduction in all.

plume out of a retail shop with a wide door have been discussed in the proposed model. So the mass flow rate of the plume $\dot{m}_p$ may be predicted by the proposed spill plume model:

$$\dot{m}_p = \begin{cases} \dot{m}_{p,a} Z > Z_{l,a} \\ \dot{m}_{p,l} H_d < Z \leqslant Z_{l,a} \\ \dot{m}_v 0 < Z \leqslant H_d \end{cases} \quad (46)$$

Heat loss to the enclosure is calculated by the similar method in the retail shop.

3.3. Transport lag time (TLT)

In most zone models, it is assumed that the smoke layer will be formed immediately after the core fire begins to burn up. Such an assumption is reasonable in a compartment with a height range of 4–5 m, but not suitable for a large space like an atrium. During an atrium fire, the propagation of the buoyant plume from the fire source to the ceiling and its spread as a ceiling jet to form smoke layer may take a time, which is much longer than the time required in a compartment space a few meters high. Hence, the transport lag time must be accounted in an atrium fire.

For a fire source with convective heat release rate of $\dot{Q}_c = \alpha_c t^p$, with a power p after ignition, a normalized transport lag time (TLT) for the plume rising to the height Z was produced by Heskestad [22]:

$$t_p^* = B^{1/(3+p)} \alpha_c^{1/(3+p)} Z^{-4/(3+p)} t \quad (47)$$

$$\text{Here} \quad B = g/c_p T_0 \rho_0 \quad (48)$$

Several models have been developed for the transport lag time induced by different types of growth fires, e.g.

- Equation by Tanaka [23], for steady power fire (not including the ceiling jet transfer time):

$$t = 1.7 \dot{Q}^{-1/3} Z^{4/3} \quad (49)$$

- Equation by Heskestad [22], for t-square fire:

$$t_2^* = B^{1/5} \alpha_c^{1/5} Z^{-4/5} t = 0.81(1 + r/z) \quad (50)$$

  where r is the distance of the ceiling jet front traveling away from the jet center.
- Equation by Delichatsios [24], for p-power fire:

$$1 + \frac{r}{Z} = \kappa \left(\frac{4}{p+3} \right)^{3/5} B^{1/5} a_c^{1/5} Z^{-4/5} t^{(3+p)/5} \quad (51)$$

These models are difficult to use to calculate the TLT directly for a common type of real fire, since the growth factor and growth power of the heat release rate of real fires are usually not known in advance. This is why the majority of present zone models haven't contained a TLT model in their codes. A universal TLT model should be able to calculate transport lag time for all common types of real fires and should be easily introduced into the code, and this is the requirement influenced the development of our present zone model. The correlations proposed by Heskestad and Delichatsios are based on the same wood crib fire burning tests which closely follow the t-square growth. Delichatsios reviewed the experimental data and then proposed the uniform correlation Eq. (51) for t^p growth fire by dimensional analysis. However, there is a discrepancy for the coefficient for t-square fires in both correlations, say 0.81 in Eq. (50) while 1.21 in Eq. (51) ($\kappa = 0.944$ according to Delichatios' work). The discrepancy might be due to the different values of the theoretical heat of combustion of pine wood used. For consistency of the correlations, we adjust the value of κ and rearrange Eq. (51) as:

$$B^{1/3} Q_c^{1/3} Z^{-4/3} t = 0.56 \left(\frac{p+3}{4} \right) \left(1 + \frac{r}{Z} \right)^{5/3} \quad (52)$$

If temporally averaging the $\dot{Q}_c^{1/3}$ up to the moment when the ceiling jet front reaches r, we get:

$$\langle \dot{Q}_c^{1/3} \rangle = \frac{3}{p+3} \dot{Q}_c^{1/3} \quad (53)$$

Substituting Eq. (53) to Eq. (52), we get a uniform correlation for all types of growth fire.

$$B^{1/3} \langle Q_c^{1/3} \rangle Z^{-4/3} t = 0.42 \left(1 + \frac{r}{Z} \right)^{5/3} \quad (54)$$

The growth exponent p does not appear in the above correlation, so we can easily calculate the TLT for the real fires, and the growth exponents are not necessary to be known in advance. It is more realistic to use the correlation, i.e., Eq. (54), to give a calculation in the zone model code. Rearranging the correlation by Tanaka, we get a constant dimensionless time defined in Eq. (47):

$$t_0^* = B^{1/3} Q_c^{1/3} Z^{-4/3} t = B^{1/3} \langle Q_c^{1/3} \rangle Z^{-4/3} t = 0.46 \quad (55)$$

Here assume $\dot{Q}_c = 0.7 \dot{Q}$.

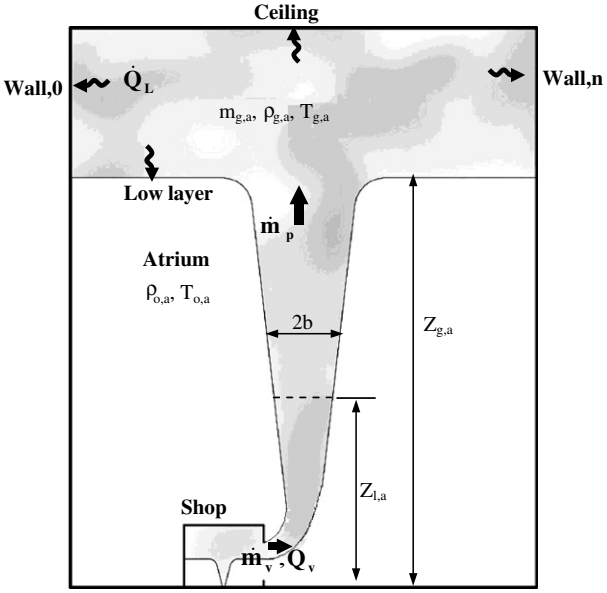

Fig. 4. Two layer analysis for natural filling in atrium due to shop fire.

A similar formation would be obtained from Eq. (55) by setting $r = 0$ in contrast to Eq. (54).

Hence, in the improved zone model, the total transport lag time after the smoke spilling out of the retail shop in the atrium, including the time to reach the ceiling of the atrium H_a and spread to the ceiling edge $\sqrt{A_{c,a}}$, is calculated by

$$t_{lag} = 0.42\left(1 + \sqrt{A_{c,a}}/H_a\right)^{5/3} B^{-1/3}\langle \dot{Q}_v^{1/3}\rangle^{-1} H_a^{4/3} \quad (56)$$

where t_{lag} should be calculated by iteration for $\langle \dot{Q}_v^{1/3}\rangle$ is the time average of $\dot{Q}_v^{1/3}$ from 0 to t_{lag} (see Fig. 4).

4. Full-scale experiments

Full-scale experiments were carried out in a retail shop mock-up located in the PolyU/USTC Atrium [13]. The dimensions of the atrium are 22.4 m (L) × 11.9 m (W) × 27.0 m (H), which is seven floors high as illustrated in Fig. 5. Four air inlets with sizes of 1.0 m × 0.25 m are located along the bottom of the east sidewall. The main atrium door with a width of 4 m is located in the center of west sidewall and the door height is adjustable, which is 2 m high in the tests. The retail shop mock-up is of 4 m (L) × 3 m (W) × 3 m (H). The frame of the mock-up is made of steel, the surfaces of the walls are lined with double-deck fireproof gypsum plaster board in 5 mm thickness, and a 5 cm air void exists between the boards.

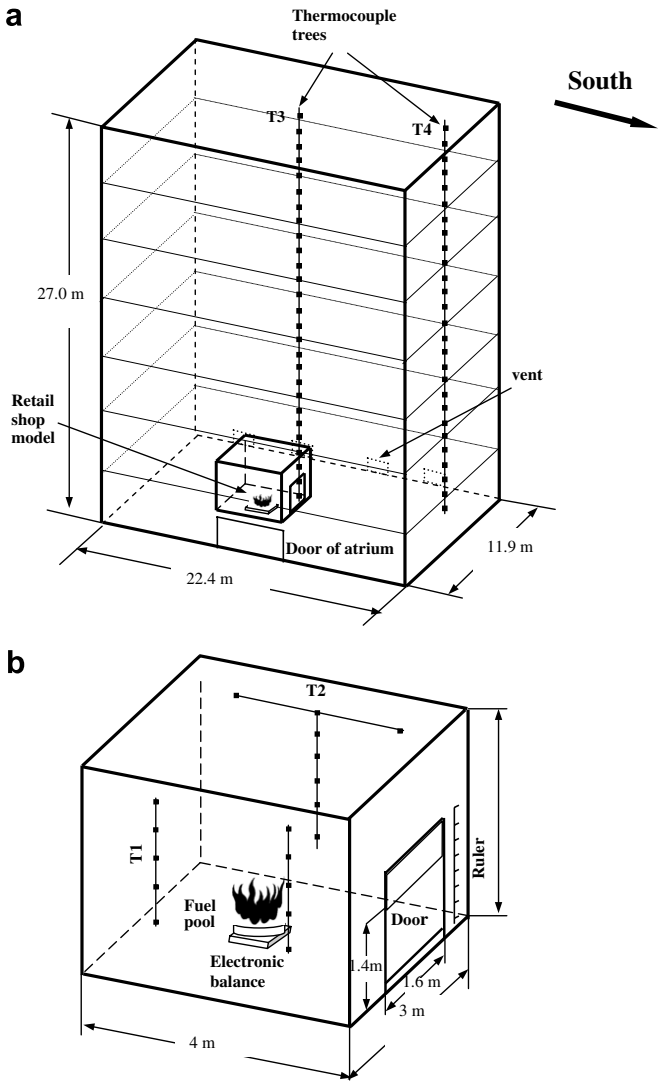

Fig. 5. Experimental setup (a) Geometry of PolyU/USTC atrium (b) Mock-up of retail shop.

Four sets of thermocouples, labeled as T1, T2, T3 and T4, were installed to measure the transient characteristic temperatures. As shown in Fig. 5(b), T1 and T2 sets are mounted on the shop wall to measure the temperature distributions inside the shop. T1 set, arranged in two vertical poles and trisecting the west wall, can be used to measure the temperatures of smoke layer at positions of 5 cm, 45 cm, 85 cm, 125 cm and 185 cm from the shop ceiling by using 10 K-type thermocouples of 1.5 mm diameter. T2 set, containing 8 K-type thermocouples of 1 mm diameter and arranged in a T-shape on the east wall, is used to provide the temperature variations in the shop. The top three thermocouples are set up at 80 cm intervals horizontally and 5 cm from the ceiling. The other five ones are arranged with vertical intervals of 35 cm, 40 cm, 40 cm, 40 cm, and 60 cm from the ceiling. From Fig. 5(a), two thermocouple trees, i.e., T3 and T4 sets, are erected to measure the temperatures inside the atrium. The T3 set is used to measure the centerline temperature of the spill plume out of the retail shop with 26 thermocouples arranged in 1 m vertical intervals and the lowest one is located 0.8 m above the ground. The T4 one contains 27 thermocouples with 1 m vertical intervals, 2 m apart from both east and south walls of the atrium, and the lowest one positioned 1 m above the floor. The thermocouples used in T3 and T4 sets are both K-type with the diameter of 0.5 mm and the cold ends of thermocouples were placed at the ground level for cold-end protection. The relative measurement errors for all sets of thermocouples are estimated as 2% for T1 and T2, and 5% for T3 and T4.

To handle the huge amount of signals and long transmission distance, two sets of data acquisition system (DAS) are developed for dealing with the fire signals. One is the central DAS, which is used to sample the signals of the electronic balance and the thermocouples of T1 and T2 inside the shop. The other is the distributed DAS [25] used for disposing the signals of T3 and T4 in the atrium. This system is developed based on filed-bus technology to minimize the signal distortion caused by electromagnetic interferences between coupling and radiation due to static, environmental and long distance transmission.

The shop was located at the place where the spill plume may be approximately located at the center of the atrium. The door opening of the retail shop was kept of 1.6 m (W) × 1.4 m (H), with a threshold of 0.3 m above the floor. A leakage of 0.05 m exists around the bottom of the walls to guarantee the uniform air supply to the burning region. The fuel has heat an enthalpy of combustion equal to 42,000 kJ/kg. Two fuel pans were of sizes 0.7 m × 0.7 m

Table 1
Experimental conditions and measured results

Tests	Pool size (m^2)	Initial temperature in retail shop $T_{0,s}$ (°C)	Initial temperature in atrium $T_{0,a}$ (°C)	Ambient temperature outside atrium (°C)	Total diesel mass (kg)	Burning time (s)	Elevation height of fire (m)	Spill plume depth at the steady stage H_v (m)
Test1	0.7 m × 0.7 m	54.0	20.8	19.0	5.3	510	0.30	0.39
Test2	0.8 m × 0.8 m	59.0	22.8	21.0	6.9	585	0.27	0.43 ~ 0.46

and 0.8 m × 0.8 m, respectively. The fuel pools were placed on an electronic balance at the central floor of the shop, slightly above the ground. The characteristic dimensions of the spill plume during the steady burning were measured with a ruler. The experimental conditions and some measured results are shown in Table 1.

The transient mass loss rate of fuel is measured by an electronic balance during the burning process within a deviation of $\dot{m}_f$ of about 5%. The heat release rate $\dot{Q}$ was calculated from the transient mass loss rate of the fuel $\dot{m}_f$, the combustion efficiency χ and the heat of combustion ΔH_c in terms of the following equation:

$$\dot{Q} = \chi \dot{m}_f \Delta H_c \tag{57}$$

Here, χ was taken as 0.9, which is confirmed by the tests of the pool fires ranging from 0.6 m by 0.6 m to 0.8 m by 0.8 m within an ISO 9705 room, with an uncertainty of 10% (2σ). Thus, the heat release rate may have a relative error of ±7.5% (or uncertainty of $2\sigma = 15\%$). The coefficient for convective heat release rate λ_c was taken as 0.7 from previous diesel fire tests. The heat release rates of both tests are shown in Fig. 6. From the figure, we can see that the burning process of diesel pool fires could be divided into three stages, i.e., a fast growing stage, a relative steady burning stage, and a final depression stage. In Test 2, the heat release rate suddenly increased at about 240 s due to a boilover occurring during the steady burning stage (The heat release rates during growth stage and steady burning stage were implemented in FDS input files as boundary conditions in time extension).

Typical temperature distributions measured in the shop and the atrium in Test 1 are shown in Figs. 7 and 8. The centerline temperatures of the spill plume measured in Test 1 are shown in Fig. 9.

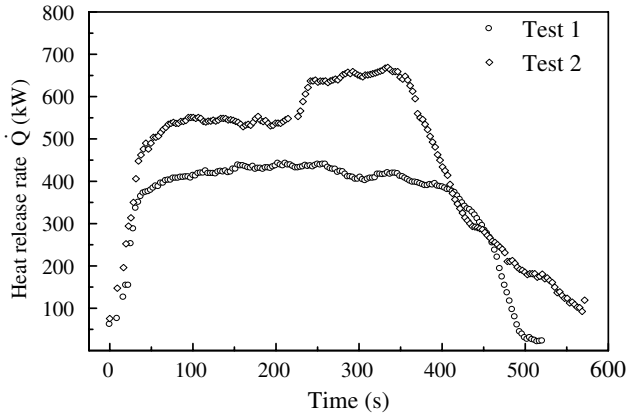

Fig. 6. Heat release rate of fire source measured in the tests.

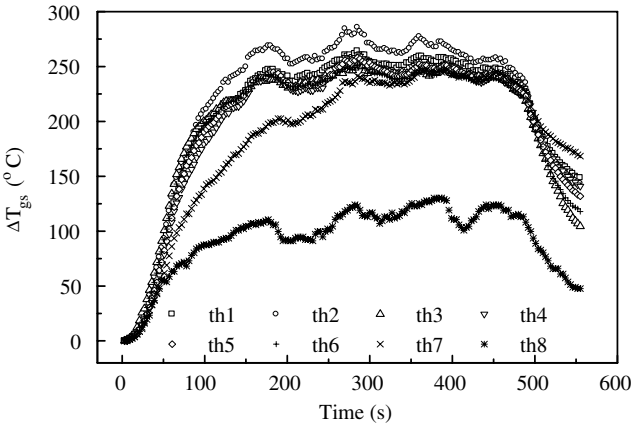

Fig. 7. Temperature rise inside retail shop measured along T1 core in Test 1.

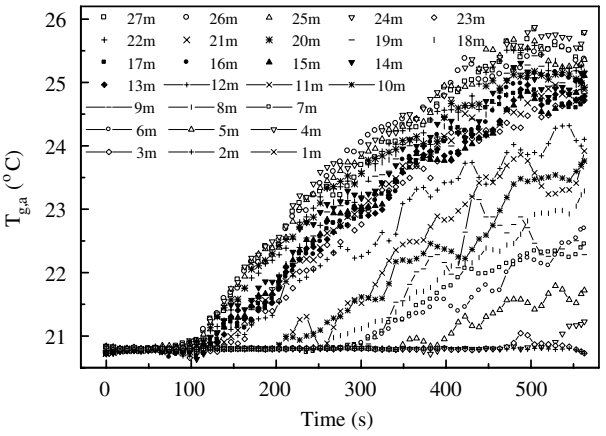

Fig. 8. Transient temperature in atrium measured along T4 core for Test 1.

5. Numerical experiments

For atrium fires, there are basically two categories of computer based approaches to simulate smoke and heat movement, i.e., zone model and field model. The zone model divides the fire environment into two spatially homogeneous volumes, i.e., a hot upper layer and a cool lower layer. Mass and energy balances are enforced for each layer with additional equations to describe relevant

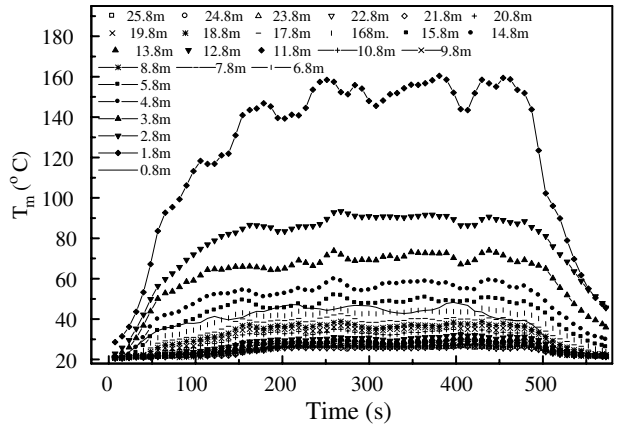

Fig. 9. Centerline temperature of spill plume measured along T3 core for Test 2.

physical processes appended to differential/algebraic equations as appropriate. The zone model is simple and computationally fast, but produces less information of the field structure of smoke movement. With the increasing capacity of computer technology, the field model has been developed extensively with the merit of CFD method. Certain works have been reported regarding the CFD modeling of fire scenarios in the literature [27–30]. Among the available CFD models, the large eddy simulation (LES) model, developed by Smagorinsky et al. [26], as an alternative to direct numerical simulation (DNS) and Reynolds Averaged Navier–Stokes (RANS) equations, simulates the large eddies of grid scale directly, models the smaller ones (subgrid scale) by subgrid-scale models, and provides detailed information on three-dimensional instantaneous velocity, turbulence, etc. Recent advances in computer performance and numerical solution have made LES model more feasible and more realistic to handle fire and smoke spread problems, although longer computational time would be required comparing to the zone model. In this study, the LES model implemented in FDS code was used to simulate the atrium fire.

5.1. Simulation by FDS code

The two full-scale tests mentioned above were simulated by the LES model implemented in FDS version 3, developed by National Institute of Standards and Technology (NIST). The turbulence is treated by means of the Smagorinsky formation. The combustion model uses the mixture fraction model, which is a conserved scalar quantity defined as the fraction of gas at a given point in the flow field originated as fuel. The radiative heat transfer is included in the model via solving the radiation transport equation by a finite volume model (FVM) for a non-scattering gray gas, using approximately 100 discrete angles. The final equation set implemented in FDS code can be used to simulate the flow phenomenon considering conservations of mass, momentum and energy for a thermally-expandable, multi-component mixture of ideal gases.

Considering the fine grid resolution against the limited computer capacity, the multi-blocking method [14] is used to establish proper meshes over the flow domain, which is a new feature of FDS code and enable users to save computational time by applying relatively fine meshes in required areas and coarse meshes elsewhere. The atrium in the study is divided into 3 mesh blocks. The first mesh block is around the shop and extended to the outer space of the compartment, 0.5 m away from the outer surfaces of the east, west, and north walls, 4.5 m away from the south wall, and 1 m away from the ceiling. The grid number in this block is $90 \times 40 \times 40$ with a resolution of 0.1 m × 0.1 m × 0.1 m. The second one is around the spill plume region $((-3,6),(-4,4),(0,27))$, the grid number is $90 \times 80 \times 120$ with a resolution of 0.1 m × 0.1 m × 0.2 m (The coordinate origin is defined as the projection point of the vertical centerline of the shop door to the ground, and the x-axis is directed to the south). The third one is the whole atrium with grid cells of $48 \times 24 \times 54$ and a resolution of 0.5 m × 0.5 m × 0.5 m.

The fire is modeled as a volumetric heat source (VHS). The heat release rate (HRR) is sampled from the measured HRRs in the tests, simplified as a growing stage and a steady burning stage with a constant HRR value. For the Test 2, the boilover stage is also considered. In FDS code, the spacial temperature variation is obtained by the animated planar slices (SLCF namelist group) and point measurement (THCP namelist group) arranged in the shop, the vertical centerline of the door, the horizontal section of the door opening height, the centerline of the spill plume, and the corresponding location of atrium. The mass flux of plume at different heights with interval 0.5 m is also calculated by THCP outputs.

5.2. Simulation by the proposed zone model and CFAST code

In the proposed zone model, the heat release rates are directly obtained from the measured curves; while in the CFAST code, the HRR curves should be sampled into several temporal points with a limited number less than 20. The thermal properties of wall structures of the retail shop and the atrium are listed in Table 2. The initial conditions are described in Table 1. Considering the temperature difference through wall structure, the initial temperature of the wall is assigned the average value of inside and outside temperatures of wall block. The boundary and initial conditions are specified same values both in the proposed zone model and CFAST code.

There are some essential differences between the proposed zone model and the CFAST code. First, the pressure equation is solved in CFAST, while constant pressure is assumed in the proposed zone model. The pressure variation should be considered carefully at the initial stage of fire in a small enclosure. However, in a relative large space

Table 2
Thermal properties of the boundary

Material (ceiling and walls)	k (w/m K)	c_p (J/kg K)	ρ (kg/m^3)	ε_w	δ (m)	Initial temperature (Test 1/Test 2) $T_{0,w}$ (°C)
Gypsum plaster (retail shop)	0.48	840	1440	0.85	0.005	38/41
Concrete (atrium)	1.2	880	2000	0.63	0.1	19.8/21.8

like an atrium, the effect of pressure variation can be neglected. Hence, the proposed model can save computing cost from this aspect. Second, the proposed model uses Heskestad's correlation for predicting the plume entrainment, considering the suitability of Heskestad's correlation to large fire involving realistic fuel packages, while the CFAST code uses McCaffrey's correlation respectively. Third, the spill plume out of the retail shop is treated as an axisymmetric plume and the mass flux is also given by the McCaffrey's correlation in CFAST, while, in the proposed model, the spill plume is predicted by the proposed spill plume model considering the three regimes. Finally, the transport lag time is included in the proposed model using the revised transport lag time model mentioned above, which is not considered in CFAST code.

The calculation steps in the proposed model are performed as follows:

First, calculate the smoke and heat movement in the retail shop

$$Z_{g,s,n}, T_{g,s,n}, T_{w,j,n} \rightarrow \left\{ \begin{array}{l} L_{m,n}, \varepsilon_{g,s,n}, G_{r,n}, k_n, v_n, l_n \rightarrow h_{j,n} \rightarrow T_{w,j,n+1/2} \rightarrow h_{j,n+1/2} \\ \rho_n, m_n \\ \dot{Q}_{n+1}, \dot{m}_{p,n+1} \end{array} \right\} \rightarrow Z_{g,s,n+1}, T_{g,s,n+1}, T_{w,j,n+1} \rightarrow H_{v,n+1}, \dot{m}_{v,n+1}, \dot{Q}_{v,n+1}$$

Second, calculate the transport lag time t_{lag} by iteration of Eq. (56), where $\langle \dot{Q}_v^{1/3} \rangle$ is obtained by the time average of $\dot{Q}_v^{1/3}$ from t_{out} to $t_{out} + t_{lag}$.

Finally, calculate the smoke spread process in the atrium, for $t > t_{out} + t_{lag}$,

$$Z_{g,a,n}, T_{g,a,n}, T_{w,j,n} \rightarrow \left\{ \begin{array}{l} L_{m,n}, \varepsilon_{g,a,n}, G_{r,n}, k_n, v_n, l_n \rightarrow h_{j,n} \rightarrow T_{w,j,n+1/2} \rightarrow h_{j,n+1/2} \\ \rho_n, m_n \\ \dot{Q}_{v,n+1}, \dot{m}_{v,n+1}, H_{v,n+1} \rightarrow Z_{o,l,n+1}, Z_{o,a,n+1}, Z_{l,a,n} \rightarrow \dot{m}_{p,n+1} \end{array} \right\} \rightarrow Z_{g,a,n+1}, T_{g,a,n+1}, T_{w,j,n+1}$$

6. Results and discussion

Based on the full-scale experiments, the smoke layers in the retail shop were observed in well-stratified form with clear interfaces in both tests. The interface in the shop slightly fluctuated in the natural filling process so that the mass exchange between the smoke layer and the lower cold air can be neglected.

The hot smoky gas firstly filled the retail shop in about 10 s, and then was driven out by the pressure difference crossing the shop door. It was observed that the smoke layer interface descended a bit lower at the beginning of the steady stage than that in the later period due to the heat expansion item described in Eq. (28). The heat expansion item generally plays a key role at the fire growth stage in a relative small enclosure; its impact gradually turns to be slight in a steady burning stage, and can be neglected in large space comparing to the mass flow items. The interface height and the temperature of the smoke layer in the shop would become relatively stable once the diesel fire becomes steady. The spill plume was steady and laminar at the door, then transferred to a line plume during the rise, and finally, an axisymmetric plume formed at the far region.

According to the records of experimenter, it took about 67 and 56 s, respectively, in both tests for the spill plume front to reach the atrium ceiling and then spread under the ceiling to form a smoke layer. Such periods are a little earlier than those correspondingly measured by the ceiling thermocouple of T4, say 80 and 63 s. It may be due to the difference of the judging criteria of the smoke front, for the former times are judged by the observation of smoke particles, while the latter ones are sensed by the sudden temperature rise of smoke. Anyhow, such transport times are relatively long and should be considered in the zone model for the large atrium case.

6.1. Characteristics of spill plume out of the shop

As observed in the experiments, the spill plume from the shop is typically divided into three regimes, i.e., the horizontal curved region out of the door, the line plume in the near field, and the axisymmetric plume in the far field. These phenomena are considered and described in the proposed model as well, i.e., Eqs. (1)–(25). According to the model, the convective heat of the spill plume $\dot{Q}_v$ can be calculated by Eq. (1) if the temperature of the smoke layer in shop and the spill depth at the door are known or by Eq. (3) if the interface height of smoke layer and the effective heat transfer coefficient are obtained in advance. Actually these two equations would give same results for the steady stage if the plume model and the heat loss through the boundary were accurate enough. Similarly, the mass flow

Table 3
Comparison of parameters produced by the proposed model and FDS code

Test No.	$\dot{Q}_v$ (kW)	$\dot{m}_v$ (kg/s)	$Z_{o,l}$ (m)	$Z_{l,a}$ (m)	$Z_{o,a}$ (m)
Test 1	130/122[a]/135[b]	0.52/0.57[a]/0.54[b]	0.60	9.63	1.93
Test 2	219/213[a]/224[b]	0.65/0.66[a]/0.67[b]	0.51	9.15	1.66

[a] Predictions by FDS code.
[b] Predictions by improved zone model.

rate out of the door $\dot{m}_v$ is calculated by Eq. (2) or Eq. (4). Here, only the steady burning stage was considered, and the key parameters of the spill plume were obtained by temporal and spatial average of the sample periods of $180 \sim 230$ s in Test 1 and $280 \sim 330$ s in Test 2, respectively. The experimental centerline temperatures of the spill plume can be obtained by averaging the measured data during these periods. The temperature of the smoke layer in the shop was obtained by the temporal and spatial average of the measured value from the thermocouples in the upper layer. Substituting the experimental parameters, the values of $\dot{Q}_v$ and $\dot{m}_v$ calculated by Eqs. (1) and (2) are shown in Table 3. The values of virtual origin $Z_{o,l}$, $Z_{o,a}$ and the critical heights $Z_{l,a}$ for spill plume transformation based on the experiments are also listed in Table 3.

Fig. 10 demonstrates the centerline temperature variations versus the atrium height produced by the experiments, the FDS code, and the proposed model. The measured centerline temperature rise ΔT_m decreases approximately with $Z - Z_{o,l}$ by exponent of -1 in the near line plume region according to Eq. (9), and about exponent of $-5/3$ in the far field according to Eq. (10). For the plume in the smoke layer region, the proposed model under-predicts the centerline temperature rise due to the entrainment

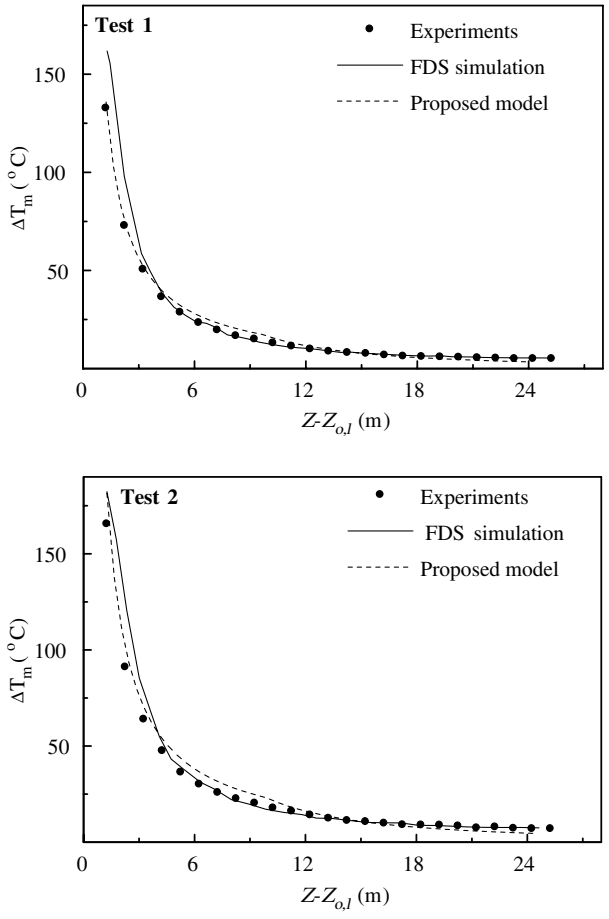

Fig. 10. Centerline temperature profiles of spill plume for Test 1 and Test 2.

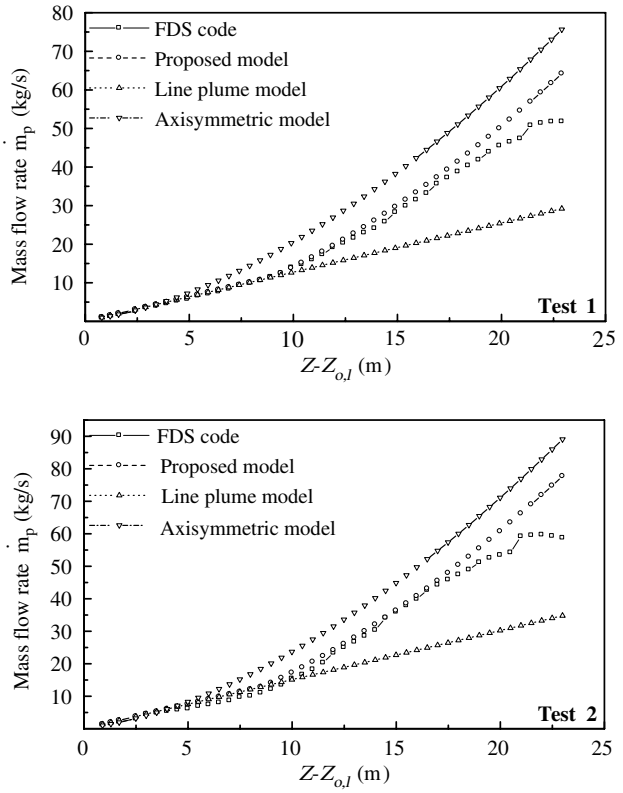

Fig. 11. Comparison of mass flow rates within models for both tests.

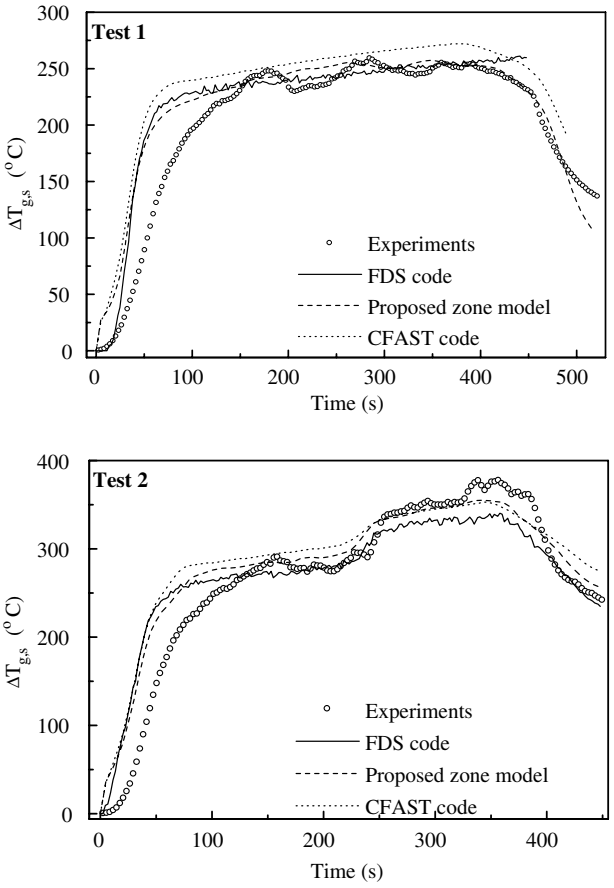

Fig. 12. Comparisons of temperature rises of smoke layer in shop.

of hot air to the plume in this region in fact. The FDS code over-predicts the ΔT_m in the near field but produces better results in the far fields than the proposed model.

Fig. 11 depicts the mass flow rates of the spill plume at a certain height predicted by the proposed model and the FDS code in steady stage for Test 1 (Fig. 11) and in boilover stage for Test 2 (Fig. 11). The figures indicate two evident regions as the spill plume moves up, i.e., the line plume regime and the far axisymmetric plume regime. The mass flow rates first linearly increase with $Z - Z_{o,l}$ in the line plume regime, and then increase with $Z - Z_{o,a}$ by $f(\exp^{5/3})$ in the far axisymmetric plume regime. As the spill plume rises to the smoke region, the temperature differences between plume and surrounding air reduce as to generate consequently less buoyance force, hence, the entrainment rates of the plume actually increase slower in the smoke layer region in FDS model than that in the proposed model, which are shown in right ends in Fig. 11. For comparison, the mass flow rate, if treating the spill plume wholly as an axisymmetric plume or a two-dimensional line plume, was predicted here. Figs. 10 and 11 show the spill plume out of a wide shop door is transferred from the line plume to the axisymmetric plume, and also demonstrate the advantage of the proposed model in properly predicting the detailed transformation from the line plume to the axisymmetric one.

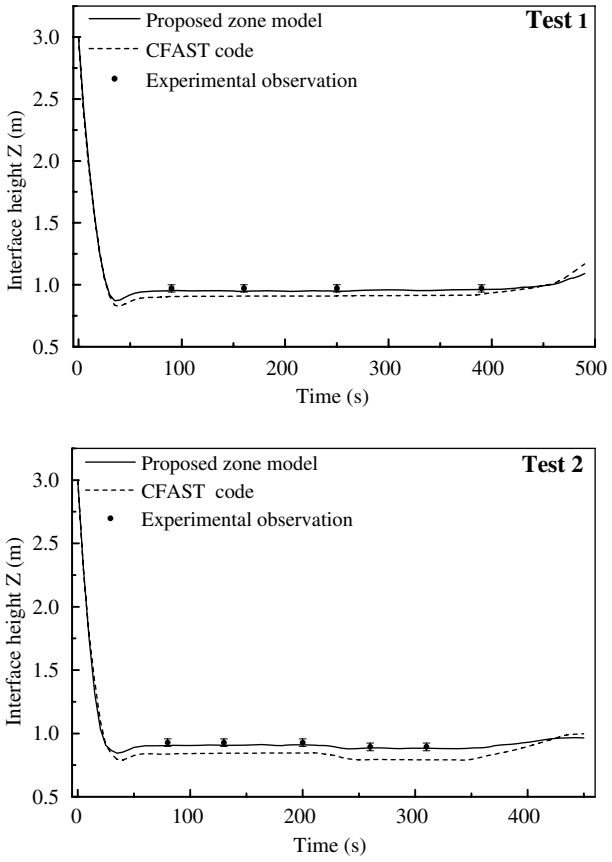

Fig. 13. Interface heights of smoke layer in retail shop for both cases.

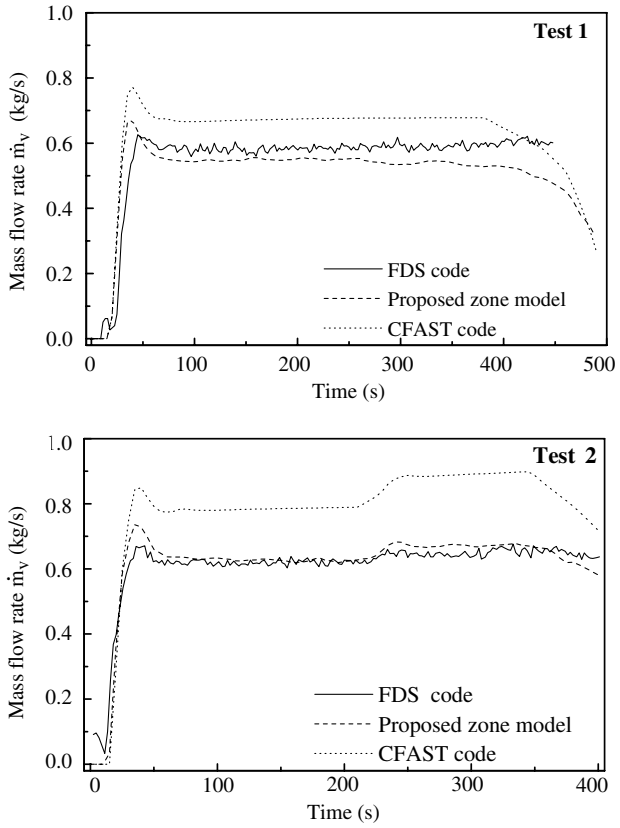

Fig. 14. Mass flow rates of spill plume at shop door for both tests.

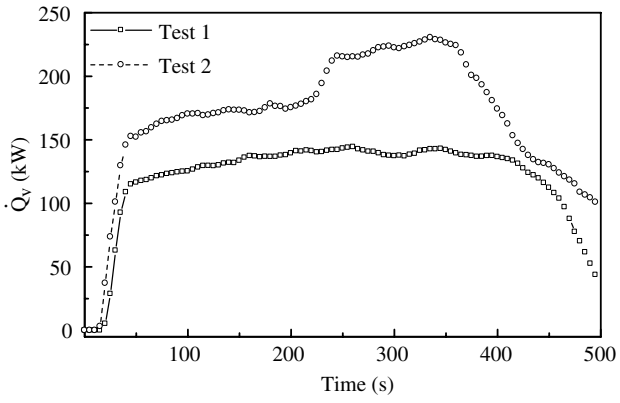

Fig. 15. Heat of spill plume for both tests.

6.2. Comparison and validation

Fig. 12 presents comparisons of the temperatures inside the shop for both tests between the prediction and the measurement. It can be seen that the results produced by the proposed model are similar to the experiments as well as the results of CFAST and FDS codes. Moreover, the maximum deviations between the proposed model and measurements in the steady stage are lower than 5% in Test 1 and 10% in Test 2. The results of the CFAST code are a little higher than the proposed model and the experiments. The predictions of the FDS code are generally in good

accordance with the proposed model and experiments except the under-estimations in the boilover stage for Test 2. It should be noted that, in the growing stage, all three models over-predict the temperature rise in similarly when compared to the experiments. Based on the observations during experiments, such deviations may be caused by two factors: (a) a vortex eddy is formed at the beginning of smoke filling inside the shop due to the downward flow along the wall so as to strongly mix the hot gases and the room air, which enhances the heat/mass exchange at the interface and cools the smoke layer, such an effect is not considered in the models used; (b) the thermal inertia of the thermocouples and the filter delay of the DAS may also enlarge the deviations.

Fig. 13 presents variation of smoke layer height inside the shop predicted by the proposed zone model and CFAST code as well as the measured ones. The smoke layer height produced by the proposed model is in a good agreement with the experiments at the steady burning stage, and the predicted spill depth at the door is similar with the measured ones, such as 0.41 m in Test 1 and 0.44 m/0.47 m in Test 2 given by the proposed model. The interface height predicted by CFAST is a little lower than that by the proposed model. It is due to the fact that different plume models were introduced in the code as mentioned before, i.e., the McCaffrey' correlation in CFAST and the Heskestad' correlation in the proposed model. Furthermore, as shown in Fig. 14, CFAST predicts more mass and heat outflow through the door to the atrium, while both the proposed model and FDS code produce similar results, which are less than those of CFAST. Fig. 15 presents the predicted heat flux of the spill plume in both cases produced by the proposed model. From Figs. 13–15, it can be seen that selecting a proper plume model is an important factor affecting the numerical accuracy. It is presumed that Heskestad's correlation is more suitable to describe relatively large fires and the details of the near field plume, since the correlation is based on large-scale experiments involving high heat release rate and realistic fuel package, which fit the situation in this study. McCaffrey's correlation is developed by measuring the average temperature and upward velocity distribution of relatively small methane fires with low-to-medium heat release rate, which may not cover the case studied here. For large fires, the turbulent structure of the flames may be different from those of a small flame. These effects should be noticed and may cause the deviation in results.

The profiles of smoke layer temperature and key heights in the atrium are shown in Figs. 16 and 17. Fig. 16 compares the transient temperature variation of the experiments with the predictions of the proposed model,

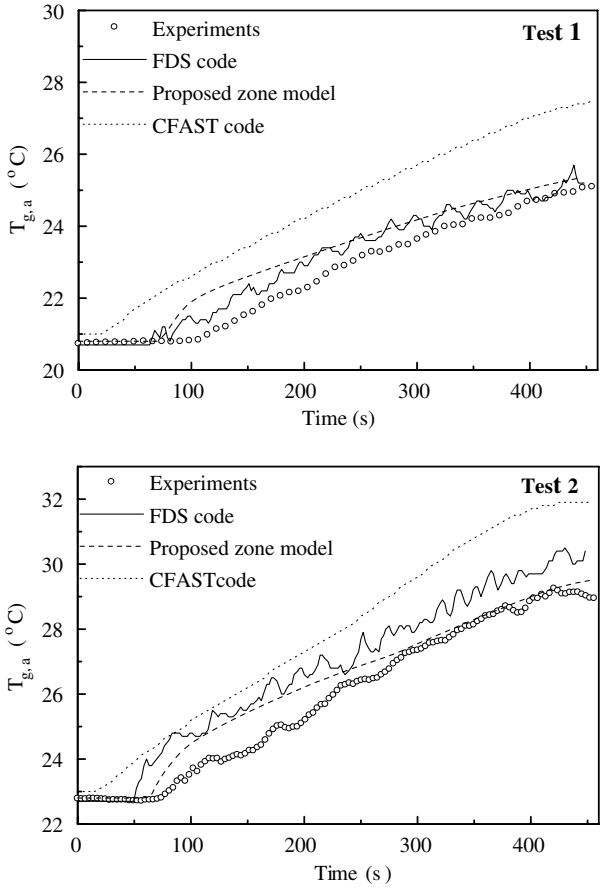

Fig. 16. Comparison of smoke layer temperature in atrium for both tests.

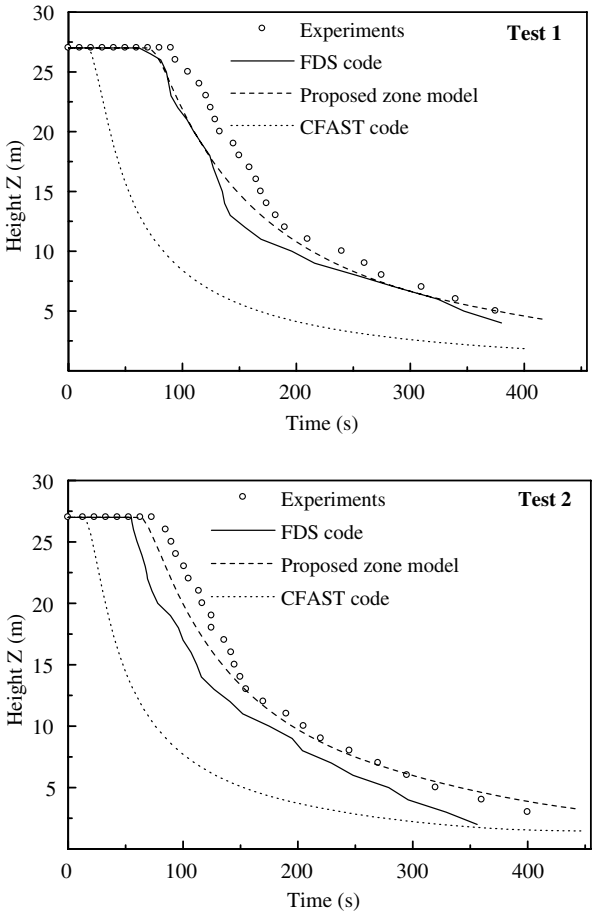

Fig. 17. Natural filling in atrium for both tests.

CFAST, and FDS codes for both tests. Fig. 17 demonstrates the comparisons of the natural filling processes in the atrium between measurements and simulations. According to Figs. 16 and 17, it can be noticed that the proposed model generally produces better predictions than the other two codes, i.e., FDS and CFAST. The temperatures predicted by the proposed model and FDS code are similar and match well to the measurements except at the beginning of the filling, which may be due to the ceiling jet entraining more cold air in experiments by the large eddy when the smoke layer is formed. The CFAST predictions deviate from the measurements at the beginning and maintain deviations to the end probably due to not considering the transport lag time. In both tests, simulations by the proposed model and FDS lead to bit earlier rises in temperature than the experiments but have similar trends with the measured data. The results of the proposed model and the FDS code get close to the measured ones at the later stages, especially in Test 2. Differences in the temperature predicted by the proposed model and FDS and measured in the experiments are found to be less 1 °C in Test 1 and 1.5 °C in Test 2. As shown in Fig. 17, the predictions produced by the proposed model and the FDS code are superior to those given by the CFAST code, which predicts an earlier natural filling due to the lack of the transport lag time impact. Besides, the natural filling curves created by CFAST are steeper than other corresponding ones due to the assumption of axisymmetric plume and the overestimation of mass flow rate by McCaffrey's correlation. On considering the transport lag time, the times for the smoke layer starting to descend are found to be close within the proposed model, the FDS code and the measurements. Particularly, in Test 2, the descending time predicted by the proposed model is almost the same with the corresponding measured one. Fig. 17 indicates that the proposed model can provide a satisfactory simulation of the natural filling compared with the experiments. Based on the similar descending trends of the measured curves and the predictions by the proposed model, two typical regions can be found in the spill plume, i.e., the line plume at near field (below 10 m) and the axisymmetric plume in the far field (over 10 m) shown in figures. Figs. 16 and 17 also present that the FDS code predicts earlier and faster natural filling in the atrium, which may be caused by the faster numerical diffusion of heat than reality due to insufficient grid resolution in the atrium block.

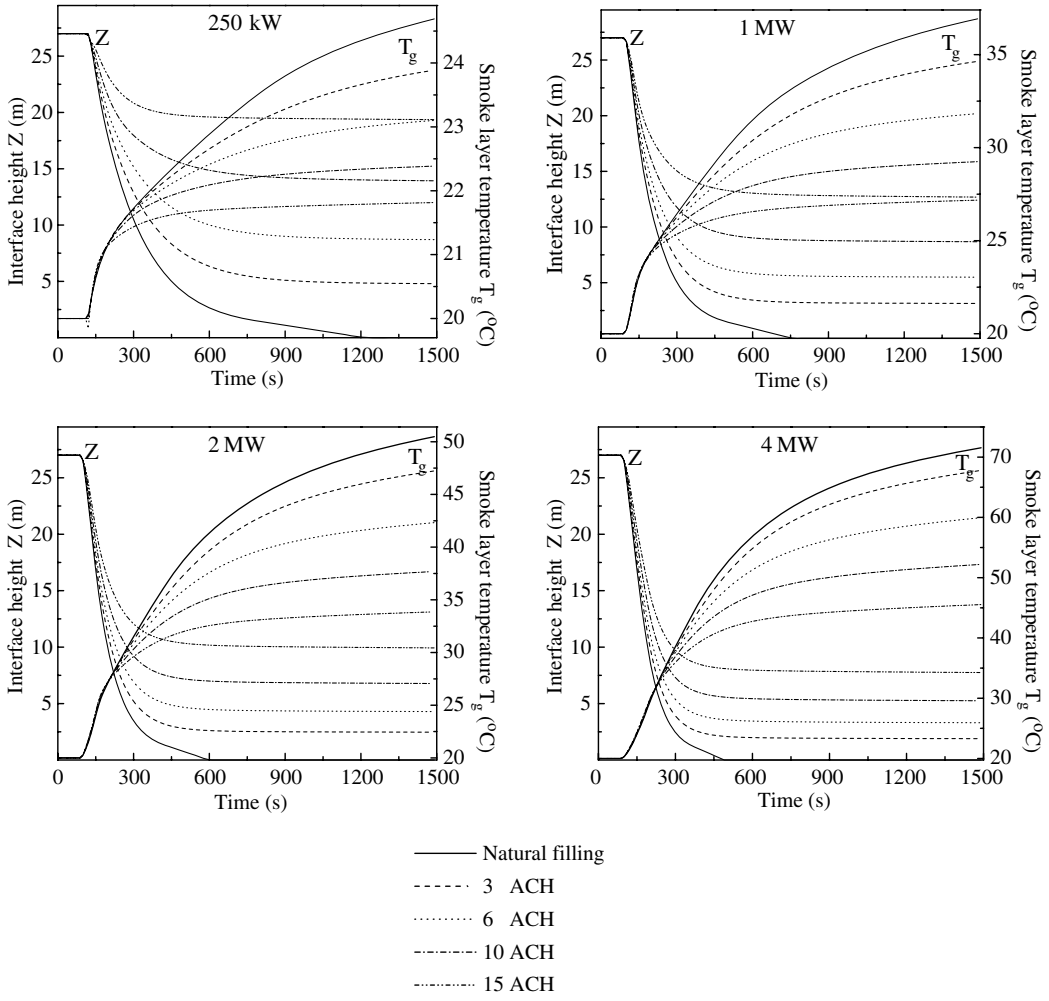

Fig. 18. Predicted interface height and smoke layer temperature in atrium under different fire sizes and mechanical exhaust rates.

Table 4
Predicted results for different fires and mechanical exhaust rates

	Shop fire size (kW)	Natural filling	3 ACH	6 ACH	10 ACH	15 ACH
Time to descend to 5 m (s)	250	450	970	N	N	N
	1000	300	380	N	N	N
	2000	260	305	430	N	N
	3000	240	270	310	N	N
Steady interface height (m)	250	0	4.8	8.8	14.0	19.4
	1000	0	3.1	5.5	8.7	12.7
	2000	0	2.5	4.3	6.8	10.0
	3000	0	1.9	3.3	5.3	7.8
Average steady smoke layer temperature (°C)	250	24.5	23.8	23.0	224	21.8
	1000	36.3	34.2	31.6	29.1	27.1
	2000	49.5	46.5	41.9	37.4	33.7
	3000	70.0	66.5	59.1	51.7	45.2

6.3. Parametric case study

The full-scale experiments and numerical simulations discussed above indicate that the natural filling in the atrium due to a retail shop fire is relatively fast, e.g., the time required for the smoke layer to descend to 5 m above ground is about 5 min in Test 2. Smoke control approaches, such as a mechanical exhaust, are important to the atrium in an emergency. To give an insight on the efficiency of mechanical exhaust in such a location due to a retail shop fire, several fire scenarios are simulated by the proposed model. The retail shop is 8 m (L) × 6 m (W) × 4 m (H) with a door of 3 m (W) × 2 m (H), which is typical of a shopping arcade in China. The atrium and the thermal properties are the same as mentioned above. The shop fires are all ultra fast t-square fires with the steady HRRs of 250 kW, 1 MW, 2 MW and 4 MW, respectively. The mechanical exhaust rate is assigned to different air changes per hour (ACH) with natural filling (zero ACH), 3ACH, 6ACH, 10ACH and 15ACH respectively. The predictions are shown as Fig. 18 and Table 4. It can be seen from the figure and the table that, with the mechanical exhaust operation, the temperature rise and descending speed of the smoke layer become slower, the temperature is lower and the smoke layer height is higher with a higher mechanical exhaust rate. The smoke layer can be kept at a key height corresponding to a desired ACH level, i.e., critical exhaust rate. In this parametric study, such rates for maintaining the smoke layer 5 m above ground are 3ACH, 6ACH, 10ACH and 10ACH corresponding to four cases with mechanical exhaust.

7. Conclusion

A detailed study on smoke movement and spill plume development in a full-scale atrium due to a retail shop fire has been reported in this paper. A simple physical model is proposed to estimate the characteristic properties of the spill plume induced by a fire in a retail shop. The transport lag time impact is also considered to predict the transport time of a spill plume to initially form a smoke layer. Introducing the spill plume model and transport lag time formation to the code, an improved zone model is developed to predict the retail shop fire in a large, tall atrium. Numerical simulations are performed by the proposed model together with the FDS and CFAST codes and compared to relevant experimental results. The following conclusions can be drawn.

Through the full-scale experiment and numerical simulation, it is found that the spill plume development in a large atrium due to a retail shop fire can be divided into three typical regions, the curved spill plume regime at the shop door, the line plume regime at the near field, and the axisymmetric plume regime at the far field.

By combining the spill plume model and the transport lag time equation, the proposed zone model can be used to predict the mass and heat movement inside the atrium with a shop fire in detail. Comparing to the predictions by the FDS and CFAST codes, it is found that for the prediction of smoke layer height and temperature rise, the proposed model performs slightly better than FDS code, especially at the growth stage, and much better than CFAST code, in which the transport lag time is not considered and the spill plume is wholly treated as an axisymmetric plume.

From the full-scale experiments and simulations, it can be seen that the natural descending of smoke in the atrium can be rapid after the occurrence of a retail shop fire. Smoke control is necessary and important for such space. The proposed model is used to carry out a parametric study on retail shop fires in an atrium under different mechanical exhaust conditions. It is found that the mechanical exhaust can slow down the speed of temperature rise and the descending of smoke layer, and may keep the smoke interface at desired height if the proper mechanical exhaust rate is maintained.

Acknowledgements

The work described in this paper was partially supported by National Key Basic Research Special Funds of China under Grant #2001CB409604, the Research Grants Council of the Hong Kong Special Administrative Region (HKSAR), China [Project No. RGC-CERG/CityU 1253/04E], and National Natural Science Foundation of China [No.50579100].

References

[1] G.O. Hansell, H.P. Morgan, Design approaches for smoke control in atrium buildings, Buildings Research Establishment Report BR 258, Building Research Establishment, UK, 1994.
[2] H.P. Morgan, J.P. Gardiner, Design principles for smoke ventilation in enclosed shopping centers, Buildings Research Establishment Report BR 186, Building Research Establishment, UK, 1990.
[3] P.H. Thomas, H.P. Morgan, The spill plume in smoke control design, Fire Saf. J. 30 (1) (1998) 21–46.

[4] J.H. Klote, J.A. Milke, Design of Smoke Management System, ASHRAE, Atlanta, GA, USA, 1992.
[5] NFPA92B, Guide for Smoke Management Systems in Malls, Atria, and Large Areas, National Fire Protection Association, Quincy, MA, USA, 2000.
[6] W.W. Jones, G.P. Forney, R.D. Peacock, P.A. Reneke, A technical reference for CFAST: an engineering tool for estimating fire and smoke transport, National Institute of Standards and Technology, NIST TN 1431, Building and Fire Research Laboratory Gaithersburg, Maryland, USA, 2000.
[7] P.H. Thomas, On the upward movement of smoke and related shopping mall problems, Fire Saf. J. 12 (1987) 191–203.
[8] M. Law, Measurements of balcony smoke flow, Fire Saf. J. 24 (1995) 189–195.
[9] B.J. McCaffrey, Momentum implications for buoyant diffusion flames, Combust. Flame 52 (2) (1983) 149–167.
[10] E.E. Zukoski, T. Kubota, B. Cetegen, Entrainment in fire plumes, Fire Saf. J. 3 (3) (1980) 07–121.
[11] G. Heskestad, Engineering relations for fire plumes, Fire Saf. J. 7 (1) (1984) 25–32.
[12] J.G. Quintiere, Fundamentals of enclosure fire zone models, J. Fire Prot. Eng. 1 (3) (1989) 99–119.
[13] W.K. Chow, N.K. Fong, The PolyU/USTC Atrium: a full-scale burning facility for atrium fire studies, in: Proc. of 1st International Symposium on Engineering Performance-Based Fire Codes, Hong Kong, 1998, pp. 186–189.
[14] K. McGrattan, Fire dynamics simulator (Version 2) – Technical reference guide, National Institute of Standards and Technology, NISTIR 6783, Gaithersburg, MD, USA, 2002.
[15] H.P. Morgan, The horizontal flow of buoyant gases toward an opening, Fire Saf. J. 11 (1986) 193–200.
[16] S.L. Lee, H.W. Emmons, A study of natural convection above a line fire, J. Fluid Mech. 11 (1961) 353–368.
[17] L.M. Yuan, G. Cox, An experimental study of some line fires, Fire Saf. J. 17 (1996) 123–139.
[18] J.G. Quintiere, B.S. Grove, Correlations fore fire plume, NIST-GCR-98-744, National Institute of Standards and Technology, Gaithersburg, MD, USA, 1998.
[19] C.L. Shi, Y.Z. Li, R. Huo, B. Yao, W.K. Chow, N.K. Fong, Mechanical Smoke Exhaust for Small Retailing Shop Fires, 2004 ASME International Mechanical Engineering Congress & Exposition, 2004, Anaheim, CA, USA, 2004.
[20] T. Sato, T. Kunimoto. Mem Faculty of Engineering, vol. 31, Kyoto University Press, 1969, 47.
[21] O. Pettersson, S.E. Magnuson, J. Thor, Fire engineering design of structures, Swedish Institute of Steel Construction, Publication, 1976.
[22] G. Heskestad, M.D. Delichatsios, The initial convective flow in fire. in: Proc. Of 7th Internationl Symposium on Combustion, Pittsburgh, PA, USA, 1979, pp. 1113–1123.
[23] T. Tanaka, T. Fujita, J. Yamaguchi, Investigation into rise time of buoyant fire plume fronts, Int. J. Eng. Perform.-Based Fire Codes 2 (1) (2000) 14–25.
[24] M.A. Delichatsios, X. Liu, C. Brescianini, Propagation of axisymmetric ceiling jet front produced by power law time growing fires, Fire Saf. J. 38 (2003) 535–551.
[25] C.L. Shi, Y.Z. Li, R. Huo, B. Yao, W.K. Chow, N.K. Fong, Mechanical smoke exhaust for small retail shop fires, Int. J. Thermal Sci. 44 (5) (2005) 477–490.
[26] J. Smagorinsky, General circulation experiments with primitive equations-I, the basic experiment, Monthly Weather Rev. 91 (1963) 99–105.
[27] Q. Chen, Computation of different k–ε models for indoor airflow computations, Numer. Heat Transf., Part B 28 (1995) 353–369.
[28] W.Z. Lu, C.M. Tam, A.Y.T. Leung, A.T. Howarth, Numerical investigation of convection heat transfer in a heated room, Numer. Heat Transf., Part A 42 (3) (2002) 233–251.
[29] W.Z. Lu, S.M. Lo, K.K. Yuen, Z. Fang, An investigation of the impact of floor setting on airflow and smoke extraction in designated refuge floor, Int. J. Comput. Fluid Dyn. 14 (2001) 327–337.
[30] W.Z. Lu, S.M. Lo, Z. Fang, K.K. Yuen, A preliminary investigation of airflow field in designated refuge floor, Build. Environ. 36 (2) (2001) 219–230.